

Orbital determination of asteroid 2011 XZ1

William Porayouw, Anshita Saini, Kai Van Brunt

July 2020

1 Abstract

Asteroids and their orbits have been well-investigated in order to monitor and classify the likelihood of a potential collision with Earth. Although positional predictions of these bodies in Keplerian motion have been developed by referencing past and prior data, fluctuations in asteroid orbit and behavior can cause considerable unreliability in the calculation of these orbits. To contribute to the current research, an orbital determination of asteroid 420302 (2011 XZ1) was calculated and defined by the six orbital elements (a , e , i , Ω , ω , M). Here we show both a quantitative and qualitative analysis of the asteroid trajectory via Method of Gauss (MoG) with the potential to improve future predictions of the asteroid's orbit. First, two-dimensional astrometric data from three sets of CCD imaging observations provided celestial coordinates of the asteroid body. Next, implementation of these coordinate values and formulaic estimations of MoG preliminaries provided general positional (r) and velocity (\dot{r}) vector information. Iteration of these calculations via computational methods ensured convergence of these values to \vec{r} and $\dot{\vec{r}}$ values with greater accuracy. Once determined, a calculation of the orbital elements presented a more accurate three-dimensional interpretation of the elliptical orbit. To calculate error propagation within the MoG iteration, uncertainty plots with a Gaussian distribution were indicated, and mean and standard deviation were given by Monte Carlo simulations.

2 Introduction

Asteroids, comets, and other (relatively) smaller bodies in the universe represent a class of debris-like materials which have formed in the universe's early age, also known as cosmic fossils. Such objects introduce the potential for further analysis of our cosmological roots, as far back as the Big Bang, and provide valuable insight into the history of the universe (Astronomy open source). Most of these asteroids orbit the space between Mars and Jupiter; however, there are few notably with orbits closer to Earth. Search campaigns dedicated to tracking orbits of these bodies has become a major international concern of NASA and its partners, both domestic and abroad. Such apprehensions are rooted in answering the critical question: how can we monitor asteroid orbits which are relatively close to that of Earth, and therefore prevent a potential catastrophic collision?

Near-Earth asteroids (NEA) are a classification described by approximately 400 known space objects with unstable orbits with the potential to either impact Earth on a collision course or be ejected from their regular orbit. Of NEAs, bodies can be further classified into more specific groups, namely Aten, Apollo, and Amor, where Aten and Apollo asteroids have perihelion distances of $q < 1.017$, and Amor has one of $1.017 < q < 1.3$ AU. Mars crossing (MC) asteroids, of which approximately 1460 members have been identified, are bodies that do not cross Earth's orbit, but intersect the orbit of Mars (The Population of Mars-Crossers).

2011 XZ1 is an Amor-class Mars crossing (MC) asteroid with current status as a NEA. With a diameter of approximately 1.085 km, a potential collision with Earth serves as a hazard, and thus

its orbit has been tracked (space reference).

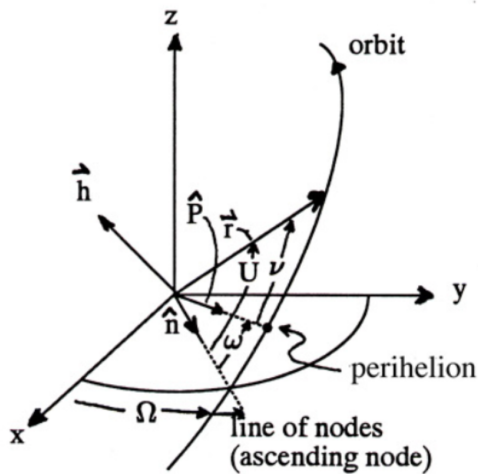


Figure 1: Orbital elements

By using two-dimensional CCD array and telescope data (i.e. right ascension and declination values, as well as astrometry) from the CWU Observatory, astrometry and photometry software, developing a Python program and simulation, three-dimensional data in the form of the orbital elements of 2011 XZ1 were calculated and underwent correction, and thus the elliptical orbit of the asteroid could be described both quantitatively and qualitatively.

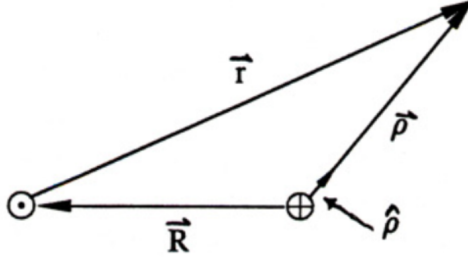


Figure 2: Fundamental triangle between the Sun, Earth, and asteroid

3 Observations and Image Processing

3.1 Data Acquisition

The following tables summarize the parameters of the instruments used for each observing session, the date of each observing session, and the results of each observing session.

Table 1: Equipment

| Network | Location | Time Zone | MPC Code | Name |
|------------------------|---|-----------|----------|--------|
| Skynet | Dark Sky Observatory | UTC-4 | W38 | DSO-14 |
| FoSSP (Friends of SSP) | Central Washington University Observatory | UTC-7 | XXX | CWU |
| (Skynet) | Perth Observatory | UTC+8 | 322 | R-COP |

| Telescope | Diameter (m) | Focal Ratio | Camera | FOV (arcmin) |
|-----------|--------------|-------------|---------------|--------------|
| C-14 | 0.356 | 12.2 | not specified | 10.5x10.5 |
| ACE 0.6m | 0.6 | 6 | FLI 4240 | 26x26 |
| 14" | 0.4 | 5.2 | | 27.6x18.6 |

Table 2: Observing Sessions

| Date and Time (UTC) | Observatory Code | Num of Images | Quality of Images |
|----------------------|------------------|---------------|---------------------|
| Fri 17 Jul 2020 7:00 | CWU | 9 | Good |
| Fri 10 Jul 2020 7:00 | W38 | 9 | Good |
| Tue 30 Jun 2020 3:00 | CWU | 9 | Good |
| Fri 25 Jun 2020 7:00 | 322 | 9 | 2 observations good |

3.2 Image Reduction

Image reduction was conducted on the computer software platform AstroImageJ (AIJ). Data was collected from a repository of observing information, including asteroid images and calibration files. After calibrating to anticipate darks, biases, and flats, the images were then aligned in order to detect the asteroid through its motion (as shown in 3).

We then plate solved the reduced but not aligned images. Using plate solve data from Astrometry.net, the right ascension and declination centroid values of the asteroid and nearby reference stars were calculated and compared to those searched in the AAVSO Photometric All-sky Survey (APASS DR9), designation II/336. Given this data, photometric analysis was conducted, where Microsoft

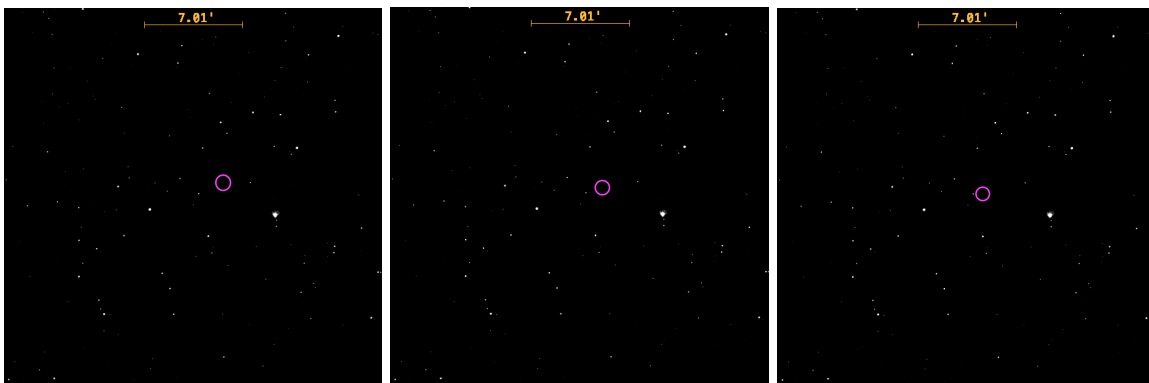


Figure 3: July 17, 2020 images showing motion of asteroid throughout observing session

excel determined the magnitude given known values for reference stars and the following equation:

$$m_{ast} - m_{star} = -2.5 \log \frac{F_{ast}}{F_{star}}$$

The mean average of m_{ast} calculated from multiple reference stars was calculated to determine the predicted magnitude of the asteroid.

4 Determination of Errors in Astrometry

To determine the root mean square uncertainties in right ascension and declination in our observations, we obtained the corresponding corr.fits file for each image from astrometry.net, which held the index and field RAs and DEC's for each of 12 reference stars in the image. By finding the average of the sum of the squares of the differences of the index and field RAs and DEC's for each star, we obtained an RMS uncertainty in RA and DEC for each image.

Table 3: Right Ascension and Declination of Asteroid 2011 XZ1

| Julian Time | Right Ascension | Declination |
|--------------------|-----------------|-------------|
| 2459025.85538902 | 20:42:19.9 | -14:05:10.8 |
| 2459030.840804759 | 20:58:49.2 | -9:36:23.5 |
| 2459040.8081781715 | 21:31:44.2 | +0:30:56.0 |
| 2459047.8783903657 | 21:53:59.9 | +7:52:03.7 |

5 Orbit Determination

5.1 Methods

In order to determine the orbit of asteroid 2011 XZ1 (2011 XZ1), The Method of Gauss (MoG) was chosen to calculate position and velocity vectors from observational data collected between June 25, 2020 and July 17, 2020. In order to take advantage of the MoG, the selected observations for implementation in the orbit determination were chosen to ensure similar intervals between the first and second, and second and third observation dates.

Table 4: Root-mean-square uncertainties in the right ascension and declination of reference stars

| UTC Date | Uncertainty in RA | Uncertainty in Dec |
|---------------|-------------------|--------------------|
| June 25, 2020 | 0.00017848 | 0.00010912 |
| June 25, 2020 | 0.00017021 | 0.00009979 |
| June 30, 2020 | 0.00011405 | 0.00019775 |
| June 30, 2020 | 0.00010339 | 0.00011578 |
| June 30, 2020 | 0.00008882 | 0.00020968 |
| July 10, 2020 | 0.00018448 | 0.00020446 |
| July 10, 2020 | 0.00020858 | 0.00018233 |
| July 10, 2020 | 0.00016567 | 0.00016753 |
| July 17, 2020 | 0.00014077 | 0.00019384 |
| July 17, 2020 | 0.00013918 | 0.00019718 |
| July 17, 2020 | 0.00013911 | 0.00019428 |

Astrometry conducted via imaging software AstroImageJ provided baseline right ascension and declination values for the orbiting body, which was then documented in a file and instituted into a Python-language software program.

We calculated the root-mean-square uncertainty in the values of RA and DEC for each image in our chosen observations and picked our final images (one from each observing session) based on which gave the lowest uncertainties.

The Python program structure for orbit determination could be described in three sections: (1) formulaic estimations of preliminary MoG values for vectors and vector constants (see Appendix C), (2) convergence of r and \dot{r} values via iteration (see Appendix B), and (3) calculation of orbital elements given converged values (see Appendix A).

It should be noted that due to asteroid 2011 XZ1’s classification as a near-Earth asteroid, MoG was considered over the Method of Laplace as a viable and more accurate approach to calculate the orbit by numerical differentiation.

In MoG, standard error propagation was not feasible with the abundance of iterative mathematical operations. Instead, to estimate uncertainty, Monte Carlo simulations was used. Assuming that the uncertainties on the α and δ for each of the observations followed a Gaussian distribution as seen in 4, 1000 values were sampled, resulting in an array of orbital elements. From the Monte Carlo simulations, the mean and standard deviation was determined for each orbital element, corresponding to the final element value and uncertainty.

To test self-consistency, the Python pyephem package was utilized, where an ephemeris of the corrected orbital elements from the middle observation predicted the right ascension and declination values of the final observation. These values were then compared to that determined by astrometry analysis of our final observation, and the percent difference with respect to the collected telescope data was calculated as 0.16973 percent for RA and 4.83411 percent for declination.

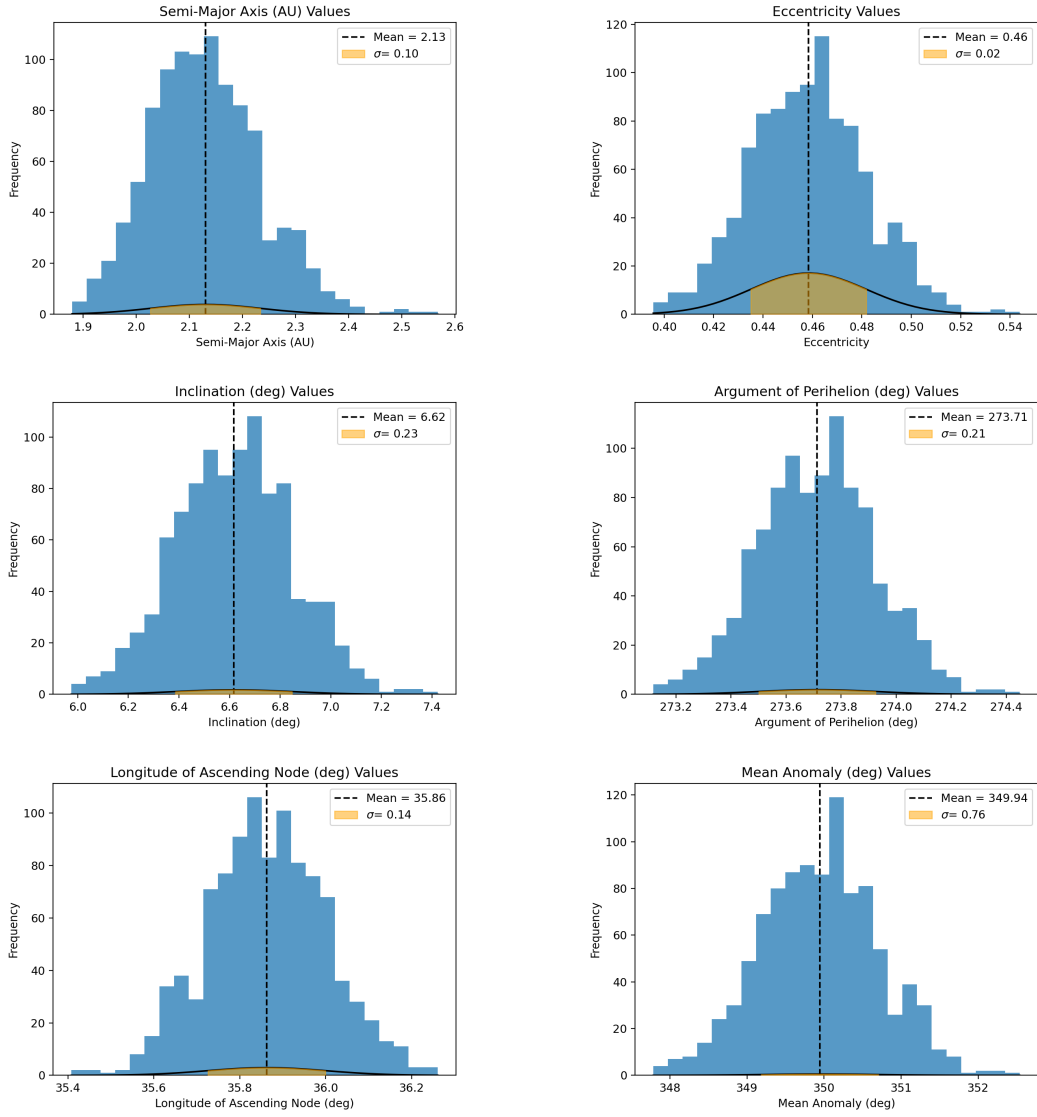


Figure 4: Results from Monte Carlo - the simulations followed a largely normal distribution.

5.2 Results

Table 5: Monte Carlo orbital elements and standard deviations

| Orbital Element | Average | Standard Deviation |
|--|---------|--------------------|
| Semimajor Axis (AU) | 2.13000 | 0.098927 |
| Eccentricity | 0.45843 | 0.022445 |
| Inclination ($^{\circ}$) | 6.61668 | 0.22161 |
| Argument of perihelion ($^{\circ}$) | 35.8621 | 0.13175 |
| Longitude of ascending node ($^{\circ}$) | 273.713 | 0.20414 |
| Mean anomaly on 07/10/20 ($^{\circ}$) | 354.704 | 0.73456 |

5.3 Orbit Visualization

A visual simulation of the asteroid's orbit confirmed the plausibility of our final orbital elements in a qualitative manner. Visual Python (VPython) was utilized to develop a program simulating the orbits of the inner Solar System beginning on June 29, 2020, recording the position vector of the orbiting bodies at arbitrary values throughout their period around the Sun. The overlap between the orbits of Mars and 2011 XZ1, as well as the latter's close proximity to the Earth at certain points of its orbit, confirm the classification of 2011 XZ1 as both an MC and NEA.

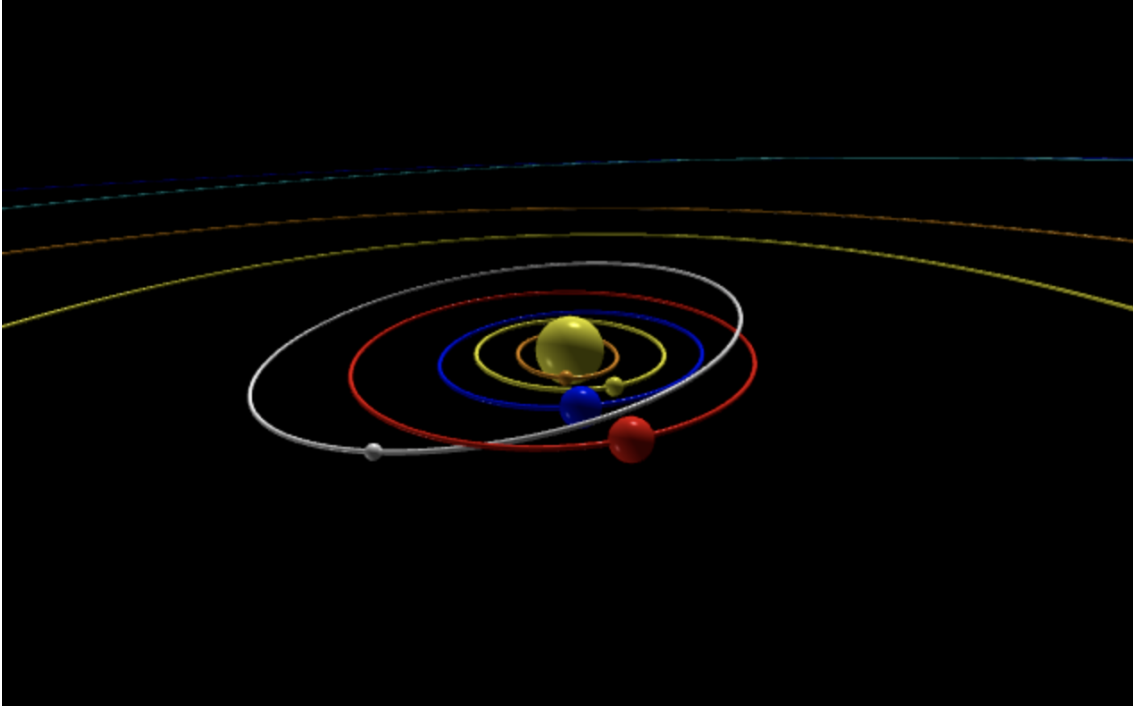


Figure 5: Edge-on view of VPython simulation

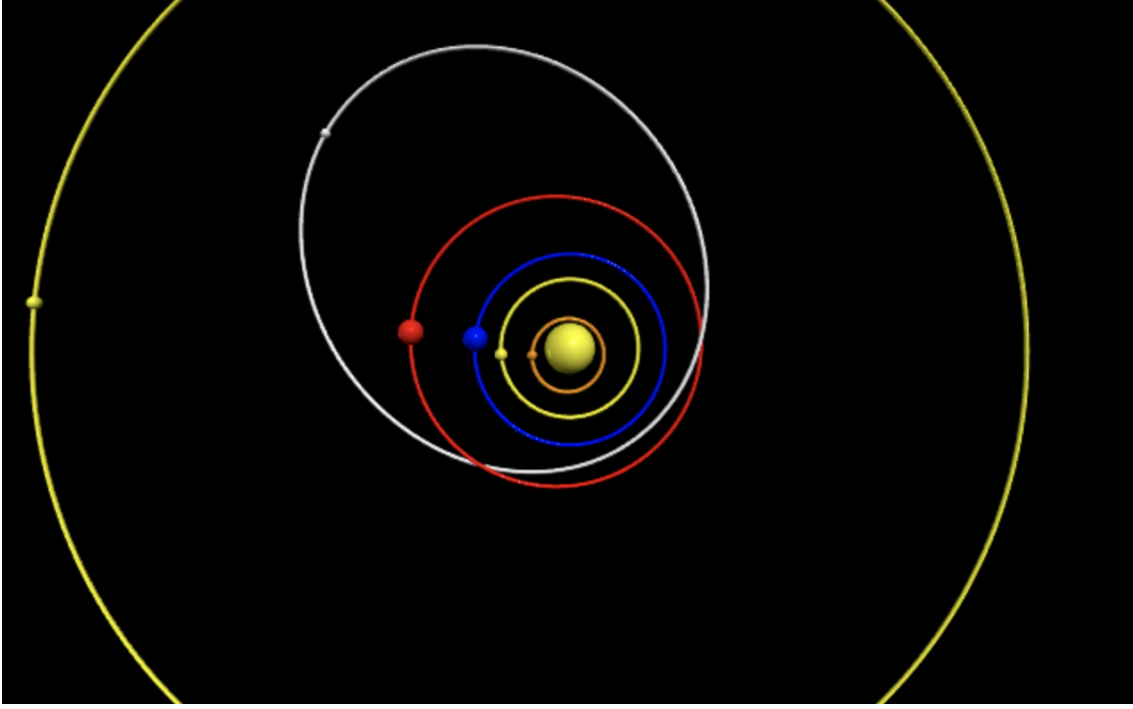


Figure 6: Head-on view of VPython simulation

5.4 Discussion

When performing the self-consistency check using pyephem data from our calculated orbital elements, and comparing that to the observational RA and declination data collected via AstroImageJ, minor difference was detected between the two compared values. Experimental software affected the quality of our results in many ways. For one of our observations, plate-solving resulted in variations in the linearity of our declination values. Moreover, not all teammates were able to arrive at correctly plate-solved images, decreasing the ability to cross-correlate results among the team. However, the values were overall within uncertainty in comparison to the values found from JPL Horizons, attesting to the overall rigor of MoG. Differential correction could be completed with a fourth observation to further improve the estimated orbit. Collecting further observations can also work in favor of improving methods of numerical differentiation and calculating more accurate values for orbital elements.

We used Slack as the primary channel for team communication outside video conferences, which we exclusively used Zoom for. We used Google Docs for the writing that was required, which included

Table 6: Comparison between our data and JPL data

| Orbital Element | JPL Data | Our Data | Percent difference |
|--|----------|----------|--------------------|
| Semimajor axis (AU) | 2.13879 | 2.13000 | 0.411% |
| Eccentricity | 0.46142 | 0.45843 | 0.650% |
| Inclination ($^{\circ}$) | 6.66679 | 6.61668 | 0.752% |
| Argument of perihelion ($^{\circ}$) | 36.2640 | 35.8621 | 1.108% |
| Longitude of ascending node ($^{\circ}$) | 273.720 | 273.713 | 0.003% |
| Mean anomaly on 07/10/2020 ($^{\circ}$) | 354.636 | 354.704 | 0.019% |

progress reports and observing requests. We also used Google Sheets to facilitate the sharing of data for the purposes of observing requests and astrometry/photometry.

Until the final OD code, the three of us did the same work independently and cross-checked with each other to ensure the accuracy of our code. For the final version of the OD code, we implemented the differential correction method and Monte Carlo method in order to improve our results. Kai primarily worked on the differential correction method, Anshita primarily worked on the Monte Carlo method, and William created the VPython visualization of the asteroid orbit. We worked on the OD report jointly.

Our team members each had very different fields of expertise which complemented each other well. Anshita had the most experience with programming from her ongoing machine learning opportunities and was able to assist the rest of us with problems in our code. William was experienced in scientific research and technical writing from and thus contributed the most to report structure, formatting, and citations. Kai had worked with calculations involving astrometry and orbital mechanics before and contributed conceptual understanding of the research. Apart from this, our team was also very compatible and sociable; there were no conflicts throughout this research process.

6 Acknowledgements

NMT Team 10 would like to thank the faculty and staff at the Summer Science Program in Astrophysics at New Mexico Tech, including Academic Director Dr. Adam Rengstorf and Associate Academic Director Dr. William Anderson, teaching assistants Amy Zhao, Zhanpei Fang, Joseph Tran, Luke Kiernan, and site director Ms. Barbara Martinez. We would also like to thank CUB Team 8, from which we obtained our July 10 data sample.

7 References

420302 (2011 XZ1). (n.d.). Retrieved July 25, 2020, from <https://www.spacereference.org/asteroid/420302-2011-xz1>

Danby, J. M. (1992). *Fundamentals of celestial mechanics* (2nd ed.). Richmond, Virginia: Willmann-Bell.

Fraknoi, A., Morrison, D., Wolff, S. C. (2017). *Astronomy*. Hong Kong: Samurai Media Limited.

Gauss, K. F. (1964). *Theory of the Motion of the Heavenly Bodies Moving about the Sun in Conic Sections*. *Mathematics of Computation*, 18(87), 525. doi:10.2307/2003798

Loff, S. (2014, April 22). *NASA's Search for Asteroids to Help Protect Earth and Understand Our History*. Retrieved July 25, 2020, from <https://www.nasa.gov/content/nasas-search-for-asteroids-to-help-protect-earth-and-understand-our-history/>

Michel, P. (2000, January 3). *The Population of Mars-Crossers: Classification and Dynamical Evolution*. *Icarus*, 145(2), 332-347. doi:10.1006/icar.2000.6358

8 Appendix A

These equations were used to determine the 6 orbital elements from the position and velocity vectors of the asteroid.

Semi-major Axis

$$a = \left(\frac{2}{|\vec{r}|} - \frac{\dot{\vec{r}} \cdot \dot{\vec{r}}}{\mu} \right)^{-1}$$

Eccentricity

$$e = \sqrt{1 - \frac{|\vec{r} \times \dot{\vec{r}}|^2}{\mu a}}$$

Inclination

$$\cos i = \frac{h_z}{|\vec{h}|}$$

Longitude of ascending node

$$\sin \Omega = \frac{h_x}{h \sin i}$$

$$\cos \Omega = -\frac{h_y}{h \sin i}$$

Argument of perihelion

$$\omega = U - \nu$$

Mean anomaly

$$M = E - e \sin E$$

9 Appendix B

Method of Gauss was used to determine the position and velocity vectors from the right ascension and declination of the asteroid given 3 observations. First, time intervals were converted to Gaussian days.

Gaussian time intervals

$$\tau_3 = k(t_3 - t_2)$$

$$\tau_1 = k(t_1 - t_2)$$

$$\tau = \tau_3 - \tau_1 = k(t_3 - t_1)$$

Light travel time correction

$$t_i = t_{o,i} - \frac{\rho_i}{c}$$

To calculate the position vector:

$$\vec{r}_2 = c_1 \vec{r}_1 + c_3 \vec{r}_3$$

where

$$\vec{r}_1 = f_1 \vec{r}_2 + g_3 \dot{\vec{r}}_2$$

$$\vec{r}_3 = f_3 \vec{r}_2 + g_3 \dot{\vec{r}}_2$$

and

$$c_1 = \frac{g_3}{f_1 g_3 - g_1 f_3}$$

$$c_3 = \frac{-g_1}{f_1 g_3 - g_1 f_3}$$

To calculate the velocity vector:

$$\dot{\vec{r}}_2 = d_1 \vec{r}_1 + d_3 \vec{r}_3$$

where

$$d_1 = \frac{-f_3}{f_1 g_3 - f_3 g_1}$$

$$d_3 = \frac{f_1}{f_1 g_3 - f_3 g_1}$$

To calculate rho, range from Earth to the asteroid:

$$d_3 = \frac{c_1}{D_1 g_3 - f_3 g_1}$$

Using these initial values, position and velocity vectors were determined using f and g series. These iterative calculations continued until the values converged.

10 Appendix C

The Scalar Equation of Lagrange was used to calculate an initial range:

$$\rho_2 = A + \frac{\mu B}{r_2^3}$$

$$r_2^8 + ar_2^6 + br_2^3 + c = 0$$

where a, b, and c are determined constants.